JOURNAL OF MATERIALS SCIENCE 21 (1986) 3912–3920

A bimodal lognormal model of the distribution of strength of carbon fibres: effects of electrodeposition of titanium di (dioctyl pyrophosphate) oxyacetate

SHI-HAU OWN*, R. V. SUBRAMANIAN, S. C. SAUNDERS‡
Department of Materials Science and Engineering, and ‡Department of Mathematics, Washington State University, Pullman, Washington 99164-2720, USA

The tensile strength distribution of Fortafil-3 carbon fibres of circular cross-section has been investigated at different gauge lengths. The unimodal Weibull, unimodal lognormal and bimodal lognormal models were tested. Estimating the model parameters by the method of maximum likelihood, and testing each model by the Kolmogorov–Smirnov goodness-of-fit statistic at prescribed levels of significance, it is found that the data for untreated unsized fibres fit a bimodal lognormal model best. The proportions of the low and high strength populations, p and q, respectively, did not show any well-defined trend with gauge length and had average values close to 0.5. But the lognormal mean for each population showed an increasing trend with decreasing gauge length. It is inferred that p and q are, respectively, related to the presence of surface flaws and internal defects, both of which probably have the same structural origin. After electrodeposition of titanium di (dioctyl pyrophosphate) oxyacetate (TDPO), the fibre strength was still best approximated by a bimodal lognormal distribution. But the weighting factor p for the weak population was reduced markedly, with a corresponding increase of q, indicating the healing of surface flaws during electrodeposition of a protective layer of TDPO. Furthermore, in contrast to the observations with untreated fibres, the lognormal means for both the low and high strength populations of the electrocoated fibres were essentially unchanged with gauge length. Changes were also indicated in the number and severity of surface flaws, caused by concurrent electrochemical processes.

1. Introduction

An important aspect of carbon fibre composite research is concerned with achieving sufficient fibre–matrix adhesion to provide efficient stress transfer without sacrificing impact toughness. Many types of surface treatments have been utilized to improve the interfacial bonding between carbon fibre and polymer matrix [1, 2]. The application of a polymer interlayer on the fibre, before composite fabrication, has been previously investigated in our laboratory. In that study, it was shown that interphase modification by electro-initiated polymerization or electrodeposition of polymers on carbon fibres results in significant improvements in both interlaminar shear strength and in impact strength of carbon-fibre–polymer composites [3, 4].

A related development in this research was the electrocoating of carbon fibres with organophosphorus compounds in the expectation that they would form an intumescent layer should the composite be exposed to fire. The tendency for "fibre lofting", that is the release of conductive carbon fibre fragments when the matrix resin is burned away, is thus minimized [5, 6]. Noteworthy among the chemicals most effective in this regard was titanium di (dioctyl pyrophosphate) oxyacetate (TDPO) which left a residual incombustible, nonconductive layer, probably of titanium dioxide, after the carbon fibre had been completely oxidized.

It was, therefore, of interest to investigate the effects of TDPO on the interfacial bonding in carbon fibre composites [7]. Surface treatments may be expected to have significant effects on fibre strength as well as on fibre–matrix adhesion. This paper examines the effects of electrodeposited TDPO on the distribution of strength of a PAN-based carbon fibre. The corresponding effects on fibre–matrix bonding are discussed in a companion paper [8] on the basis of a new statistical theory for the distribution of interfacial shear strength. A significant feature of the theory is that it utilizes the gauge-length dependent distribution of fibre fracture stress (discussed in this paper), for the deduction of the distribution of the interfacial shear strength.

2. Experimental details

2.1. Materials

TDPO, shown in Fig. 1, was obtained from Kenrich

* *Present address:* Department of Aeronautics, Naval Postgraduate School, Monterey, California 93943, USA.

0022–2461/86 $03.00 + .12

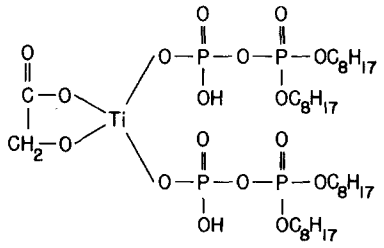

Figure 1 Chemical structure of titanium di (dioctyl pyrophosphate) oxyacetate.

Petrochemical, Inc, (Bayonne, New Jersey) as KR-138S, a solution in isopropanol, with an active content of 80%. The carbon fibre Fortafil-3 was obtained from Great Lakes Corporation (Elizabethton, Tennessee), as unsized fibre of circular cross-section with no surface treatment and with 40 000 filaments per tow, without twist. The Young's modulus of the fibre was 200 GPa (30×10^6 psi).

2.2. Electrodeposition

The solution of TDPO for electrodeposition was prepared by slow addition of triethylamine (20 g) to 40 g KR-138S until the pH was between 6 and 8. The clear solution was added to 2000 g distilled water with stirring.

The carbon fibre, mounted on an H-frame, was used as the anode with stainless steel cathodes placed on either side of the fibres to facilitate uniform electrodeposition. A Micronta variable d.c. power supply from Radio Shack with a voltage range of 0 to 24 V was used for electrodeposition.

The fibres were left to soak in the electrolyte solution for 4 min before applying the voltage to the electrodes. Three sets of electrodeposition conditions were applied. Specimens TITAO2 and TITAO4 were both obtained by electrodeposition at 0.66 A and 7.4 V for 60 sec; but the latter was washed for 5 min in water after the anodic deposition process. For specimens TITAO3, the conditions were altered to 2.8 A and 20 V for 180 sec, with washing in distilled water for 5 min after electrodeposition.

2.3. Fibre strength measurement

Fibre diameter was measured by an American Optical microscope (type I-60) using a Vickers image-splitting eyepiece. The tensile strength of the fibres was measured using a tensile testing machine constructed in-house following the specification given by Schile and Rasica [9]. The fibre was glued across the diameter of a circular hole cut in the middle of a rectangular paper frame which was then mounted between the moving and stationary crossheads of the tensile tester. The crosshead was moved at a constant rate of 1 mm min^{-1}. A temperature-compensated, strain-gauge type cell was mounted on the stationary crosshead. An electronic bridge circuit was used to monitor the load cell. It responds only to load components in the direction of the fibre axis. The gauge length of the fibre specimen was varied by changing the diameter of the hole in the paper frame across which it was fixed on the circumference. The sides of the paper frame were cut so that the fibre was loaded by the crosshead movement. The load readings were recorded on a chart by a recorder. At least 40 fibre specimens were tested for each set of measurements at a particular gauge length, for each surface treatment. The gauge lengths selected were at least four of 4.76, 6.35, 9.54, 12.7, 22.4 and 40 mm.

2.4. Modelling of the strength distribution and the estimation of parameters

The sequence of steps in the modelling of fibre strength was first to select possible strength models, second, estimate the parameters by the method of maximum likelihood, third, test each model using the Kolmogorov–Smirnov goodness-of-fit statistic at a prescribed level of significance [10] and finally select from among the models those that are acceptable, choosing the one with the most plausible physical foundations. The strength models considered are the unimodal Weibull, unimodal lognormal, or bimodal lognormal models [11]. The objective was to compare the two most widely accepted unimodal distributions with a bimodal distribution that is easily handled. (We use the word bimodal-lognormal to mean a mixture of two separate lognormal populations.)

The unimodal Weibull model is based on the weakest link theory assuming a power law of flaw distribution. The probability (Pr) of fibre strength Σ less than σ in a Weibull model is given by Equation 1:

$$\Pr(\Sigma < \sigma) = 1 - \exp\left[-\left(\frac{\sigma}{\beta}\right)^{\alpha}\right] \quad \text{for } \sigma > 0 \quad (1)$$

where α is the modulus (or shape parameter) and β is the scale parameter for Weibull distribution. It is assumed that the scale parameter, β, depends on the gauge length of the test specimen, while the Weibull modulus, α, only depends on the material under test. The probability density function is obtained by differentiation of the cumulative distribution (Equation 1), yielding Equation 2 below:

$$W(x:\alpha, \beta) = \left(\frac{\alpha}{\beta}\right)\left(\frac{x}{\beta}\right)^{\alpha-1} \exp\left[-\left(\frac{x}{\beta}\right)^{\alpha}\right] \quad (2)$$

The lognormal distribution has the following density function:

$$f(x:\mu, \sigma) = \frac{1}{(2\pi)^{1/2}\sigma x} \exp\left\{-\frac{[\ln(x) - \mu]^2}{2\sigma^2}\right\} \quad \text{for } x > 0 \quad (3)$$

where μ is the lognormal mean and σ is the lognormal standard deviation. The lognormal distribution would follow whenever the random strength, x, is determined from the multiplicative effect of processing conditions and manufacturing variations, assuming such effects are positive and independent.

The bimodal lognormal model arises through the mixing of two lognormal populations with proportions p and q, namely:

$$f(x) = pf_1(x:\mu_1, \sigma_1) + qf_2(x:\mu_2, \sigma_2) \quad (4)$$

where $p + q = 1$.

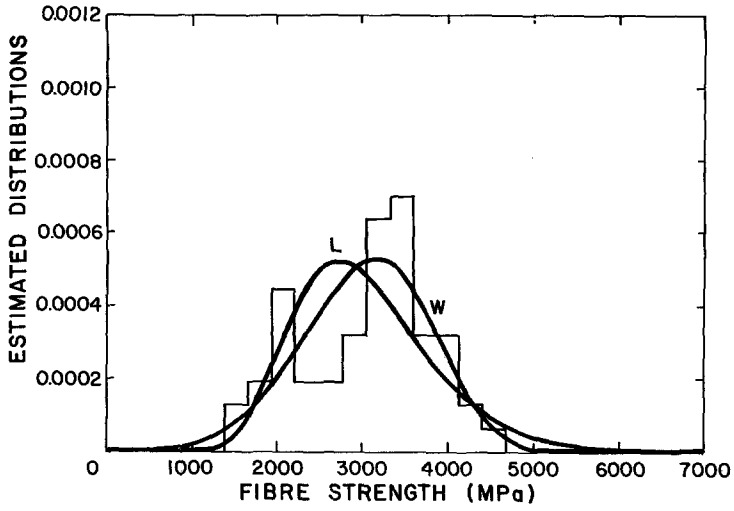

Figure 2 Empirical histogram, lognormal model (L) and Weibull model (W) for the strength distribution of F3UTUS fibre at 40 mm gauge length.

3. Results

3.1. Empirical strength distribution

The fibres used in strength tests as well as in single filament composite tests were Fortafil 3 untreated, unsized (F3UTUS) carbon fibres with a circular cross-section. Specific mention is made here of the circular cross-section of the experimental fibres since the commercial Fortafil fibres, obtained until recently, have had a dumb-bell cross-section. The mean diameter, measured along the length of a fibre was 8.02 $\pm$ 0.24 μm and among many fibres of a tow was 7.93 $\pm$ 0.49 μm. The latter value was used to calculate fibre strength since specimens were obtained at random from different filaments in the tow. Washing the F3UTUS fibres with distilled water was found to produce negligible change in strength. Consequently these fibres, as-received, were used as the control in evaluation of the effects of electrocoating in an aqueous medium.

Fig. 2 shows the histogram and two models for the strength distribution of F3UTUS fibres at 40 mm gauge length. It is clear that neither the unimodal lognormal nor the unimodal Weibull model fits the empirical histogram very well. The same observation can be made from a comparison of the empirical cumulative distribution functions (ECDF) for the fibre strength (Fig. 3), and from an examination of the estimated parameters for the normal, lognormal and Weibull models which are tabulated for the F3UTUS fibre at various gauge lengths (Table 1). The standard deviations in the fibre strength are no less than 20 to 25% of the average fibre strength; they also show an increasing trend with decreasing gauge length.

In contrast to Fig. 3, the ECDF in Fig. 4 shows a good fit with a bimodal lognormal model having the form of Equation 4, where μ_1, σ_1 and p are now, respectively, the lognormal mean, lognormal standard deviation, and proportion of the low strength population, and μ_2, σ_2 and q are the corresponding parameters for the high strength population. Similarly a good agreement with the experimental data at other gauge lengths with the bimodal lognormal model is seen, even though a slight deviation is observed at the lowest gauge length, possibly caused by larger errors of measurement at the shorter gauge length.

The goodness-of-fit is clearly higher, however, for the bimodal lognormal model than for the other models. The estimated parameters for the bimodal lognormal model for the strength of the experimental fibres are given in Table II, and the levels of significance in Table III. A significant feature of these results, seen more clearly in Fig. 5, is the decreasing trend of the lognormal mean with increasing gauge length, for both the high and low strength populations. At the same time, the proportions of the low and high strength populations, p and q, respectively, do not show any well-defined trend. Over the whole

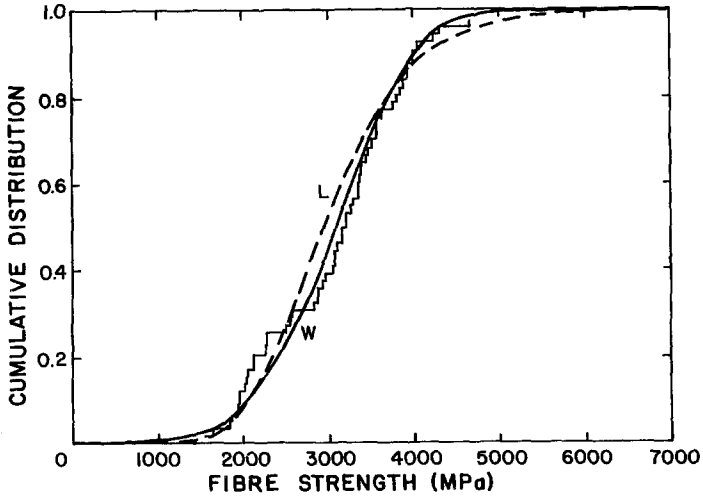

Figure 3 Empirical cumulative distribution function, lognormal model (L) and Weibull model (W) for the strength of F3UTUS carbon fibre at 40 mm gauge length.

TABLE I Estimated parameters for normal model, lognormal model and Weibull model of the strength (MPa) of F3UTUS carbon fibre at different gauge lengths

Parameters	Gauge length (mm)					
	4.76	6.35	9.54	12.7	22.4	40
Size	57	54	65	52	100	57
Mean	3780	3850	3490	3480	2830	3030
Deviation	952	851	858	745	725	755
Log. Mean	8.21	8.16	8.13	8.13	7.91	7.98
Log. Dev.	0.258	0.238	0.251	0.220	0.272	0.270
Weibull alpha	4.27	5.20	4.41	5.15	4.32	4.67
Weibull beta	4140	4190	3820	3780	3100	3320
Exp. (Log Mean)	3660	3500	3380	3400	2730	2930

range of gauge lengths studied, the average value of p is 0.48 and that of q is 0.52.

3.2. Electrocoated fibres

The strengths of fibres electrocoated by TDPO (TITAO2, TITAO3, and TITAO4) also show the best fit to a bimodal lognormal distribution, as in Fig. 6 for example. However, in stark contrast to the results obtained for untreated fibre, the lognormal mean showed little variation with gauge length for the coated fibres. Furthermore, the low and high strength proportions were strongly gauge length dependent, with p decreasing (and q increasing) with the decreasing gauge length (Tables IV to VI). A double logarithmic plot of q against gauge length is shown in Fig. 7 for TITAO2. The linear regression line has a slope of 1.59 which indicates the gauge length sensitivity. The linear relationship is given by $\ln q = \ln a - bL$, where $\ln a = 2.86$ and $b = 1.59$. The other two experimental fibres, also electrocoated with TDPO, but under different conditions, showed the same dependence, but with different gauge length sensitivities. Thus, for TITAO3 fibres, $\ln a = 0.92$ and $b = 0.81$; and for TITAO4 fibres $\ln a = 1.01$ and $b = 0.70$.

The most salient features of the results can thus be summarized as in Table VII. A bimodal distribution fits the data best; and the effects of electrocoating are reflected in the marked variations in the proportions of the weak and strong populations, and in the differences in gauge length sensitivity.

4. Discussion

4.1. Bimodal distribution of fibre strength

Carbon fibres fall into the class of brittle materials exhibiting a broad distribution of tensile strength, with a marked dependence of measured strengths on gauge length. The theory most widely applied to explain the data is that of Weibull [12], based on the concept of the weakest link in the specimen determining the observed strength.

It is noteworthy that past investigations have treated the fibre strength distribution as unimodal, in spite of clear indications from experimental data that the distributions are multimodal [13, 14]. A recent exception is the approach of Beetz [15] who has presented a new statistical analysis which allows the possibility of multiple modes of failure. Beetz has used a mixture of two Weibull distributions and applied this bimodal distribution to strengths of pitch-based Thornel-P fibres.

It is important to obtain a reliable prediction of fibre strength at gauge lengths of the order of the critical length for stress transfer (0 to 1 mm) in order to predict the performance strengths of fibre-reinforced composites. Since fibre strength data at such short gauge lengths cannot be determined experimentally, proper modelling and analysis of the strength data for the experimentally accessible longer gauge lengths is required to make a reliable prediction of strength at very low gauge lengths. The unimodal approximation underestimates the shape parameter (in the Weibull

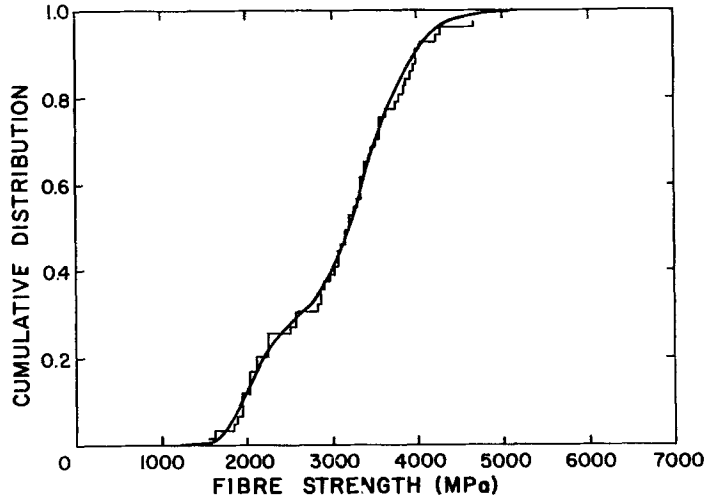

Figure 4 Empirical cumulative distribution function and bimodal lognormal model for the strength of F3UTUS carbon fibre at 40 mm gauge length.

TABLE II Parameters for the bimodal lognormal model of the strength (MPa) of F3UTUS carbon fibre at different gauge lengths

Parameters	Gauge length (mm)					
	4.76	6.35	9.54	12.7	22.4	40
Size	57	54	65	52	100	57
Log mean (1)	8.00	7.96	7.93	7.94	7.70	7.64
Log Dev. (1)	0.183	0.151	0.156	0.135	0.199	0.145
Log Mean (2)	8.40	8.38	8.35	8.32	8.12	8.14
Log Dev. (2)	0.147	0.109	0.111	0.099	0.136	0.125
p	0491	0.352	0.538	0.500	0.500	–
q	0.509	0.648	0.462	0.500	0.500	–

TABLE III Significance levels in the Kolmogorov–Smirnov goodness-of-fit test for different models of strength of carbon fibres

Fibre	Weibull	Lognormal	Bimodal lognormal
F3UTUS/4.76 mm	0.500	0.920	0.920
F3UTUS/6.35 mm	0.380	0.003	0.940
F3UTUS/9.54 mm	0.290	0.530	0.850
F3UTUS/12.7 mm	0.370	0.390	0.920
F3UTUS/22.4 mm	0.220	0.770	0.460
TITAO2/6.35 mm	0.590	0.330	0.990
TITAO2/9.54 mm	0.200	0.420	0.850
TITAO2/12.7 mm	0.460	0.680	0.520
TITAO2/15.9 mm	0.156	0.985	0.770
TITAO3/4.76 mm	0.460	0.987	0.984
TITAO3/6.35 mm	0.500	0.100	0.940
TITAO3/9.54 mm	0.150	0.810	0.890
TITAO3/12.7 mm	0.760	0.570	0.200
TITAO4/4.76 mm	0.380	0.920	0.990
TITAO4/6.35 mm	0.700	0.630	0.990
TITAO4/9.54 mm	0.530	0.580	0.750
TITAO4/12.7 mm	0.420	0.580	0.966

treatment), and results in overestimation of the mean strength extrapolated to short gauge lengths. The bimodal analysis was shown by Beetz to yield a better set of Weibull parameters, thus allowing more accurate estimates of mean fibre strengths at short gauge lengths [15].

The fit of our results to a bimodal distribution of fibre strengths is thus consistent with other observations with carbon fibres. The use of a lognormal distribution provides an alternative, and probably easier, way to treat the data compared to Beetz's analysis using Weibull statistics.

It is interesting to note that the fractions p and q, respectively, of the low and high strength portions do not change with untreated fibre, and that each is close to 0.5 within the range of gauge lengths employed. It can be surmised that the two strength populations are characterized by two different types of flaws of different severity, the more severe type causing the weaker population and vice versa. If N_1 and N_2 are, respectively, the total number of the more severe and less severe flaws, and $G_1(l)$ and $G_2(l)$ are, respectively, the distribution of interflaw spacing for the two types, then one can write p and q

$$p = N_1 G_1(l)/[N_1 G_1(l) + N_2 G_2(l)],$$

$$q = 1 - p$$

as functions of l.

The strength distribution of the mixed population, $f(x)$, is given by Equation (4).

Since p and q are observed to be virtually constant within the range of tested gauge lengths, some inferences can be drawn. In the case when both the interflaw spacings are far less than the gauge length, then it might be inferred that the average spacing of both types of flaws are about the same. Or if the interflaw spacings fall in the range of the tested gauge lengths, then the distribution of interflaw spacing is the same for both types of defects.

The presence of internal defects in addition to surface flaws in carbon fibres, including Fortafil fibres, is well documented [16]. Recently, Bennett *et al.* [17] have shown that failure of PAN-based carbon fibres was initiated both at internal and surface flaws, and that when such flaws did initiate failure, they showed evidence of large misoriented crystallites in the walls of the flaws. Thus they concluded that it is the presence of the misoriented crystallites rather than the

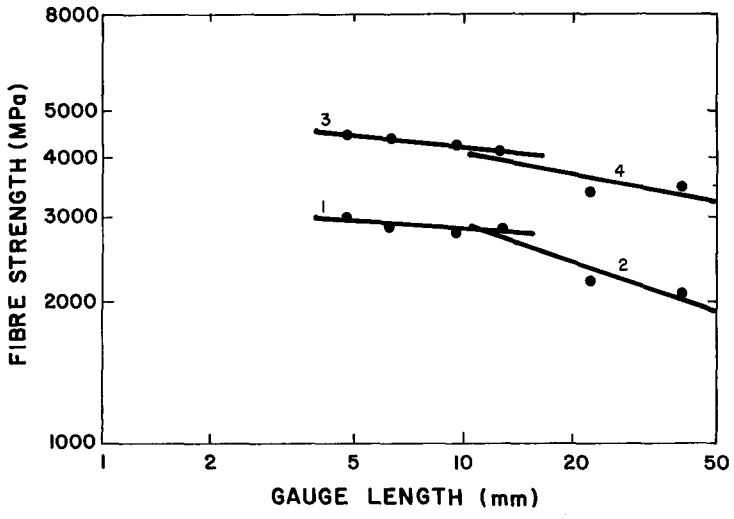

Figure 5 Gauge length dependence of the lognormal mean parameters for the bimodal lognormal model of F3UTUS carbon fibre. Low strength population: curves 1 and 2; high strength population: curves 3 and 4.

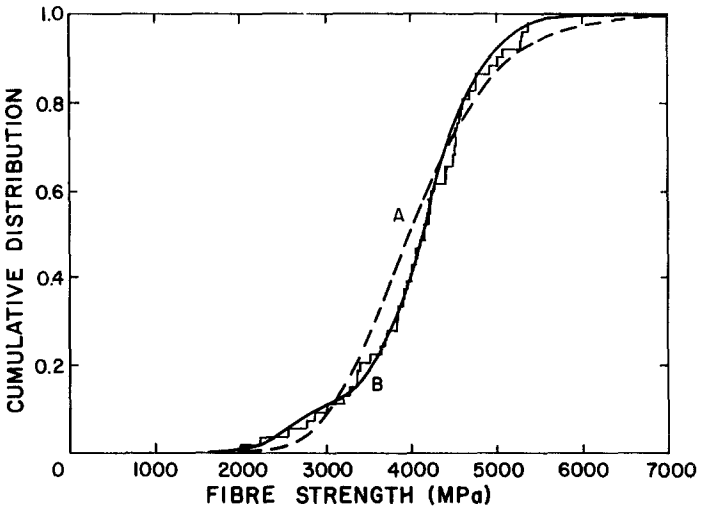

Figure 6 Empirical cumulative distribution function, unimodal lognormal model (A) and bimodal lognormal model (B) for the strength of TITAO2 carbon fibre at 6.35 mm gauge length.

flaws themselves which determined whether or not tensile failure will occur. Both types of effective flaws were therefore seen to have the same structural origin, namely the occurrence of misoriented crystallites. It is possible that the Fortafil fibres, also PAN-based, possess similar structural features and flaws. It is then not unreasonable to infer from our results that the proportions of both types of flaws should remain unchanged at different gauge lengths of the untreated fibre.

4.2. Effects of electrocoating

It was pointed out earlier that the most striking effect of electrodeposition of TDPO is the reduction of the weak population fraction p, with corresponding increase in q, the proportion of strong population, as illustrated in Figs 8 to 10. The estimated distributions of fibre strength are presented in these figures, calculated from results in Tables II, IV, V and VI. In these calculations, q for untreated fibre, was averaged over the four lowest gauge lengths measured (4.76 to 12.7 mm) since there was no significant change in this fraction with gauge length. However, in the case of electrocoated fibres, for which q varied with gauge length, the values of 6.35 mm gauge length were used in constructing these for comparison with untreated fibre. Similarly, the lognormal parameters used in these calculations were the averages over four shortest gauge lengths since there was very little difference in these values at these gauge lengths.

Unmistakably, as seen in Fig. 8 the low strength population is reduced and the high strength population increased by electrodeposition (TITAO2), compared to untreated fibre (F3UTUS). This reduction in weak population is not so marked for TITAO3 fibres electrocoated at higher current and voltage (Fig. 9). It can also be noted in this figure that the high strength extension of the distribution is shrunk by electrodeposition, indicating that severe flaws might have been created, or existing flaws made more severe by the more severe conditions of electrodeposition adopted in preparing TITAO3 fibres. Furthermore, it is interesting to see indications of the effects of washing, by comparing the density functions for TITAO2 (unwashed) and TITAO4 (washed) fibres, both electrocoated under the same conditions (Fig. 10). The influence of the protective layer of coating retained in the unwashed fibre is seen in the lower proportion of the weak population and the increased proportion of strong population for TITAO2 fibres.

The observed changes in the trends for p and q for electrocoated fibres can now be discussed on the basis

TABLE V Parameters for the bimodal lognormal model of the strength (MPa) of TITAO3 carbon fibre at different gauge lengths

Parameters	Gauge lengths (mm)				
	4.76	6.35	9.54	12.7	Average
Size	40	49	40	48	44
Log Mean (1)	7.81	7.82	8.04	8.04	7.92
Log Dev. (1)	0.127	0.197	0.113	0.193	0.158
Log Mean (2)	8.24	8.19	8.32	8.28	8.26
Log Dev. (2)	0.117	0.106	0.100	0.090	0.103
p	0.325	0.408	0.600	0.688	–
q	0.675	0.592	0.400	0.312	–

TABLE IV Parameters for the bimodal lognormal model of the strength (MPa) of TITAO2 carbon fibre at different gauge lengths

Parameters	Gauge length (mm)				
	6.35	9.54	12.7	15.87	Average
Size	52	45	43	46	46
Log Mean (1)	7.88	7.78	7.89	7.72	7.82
Log Dev. (1)	0.153	0.125	0.182	0.185	0.161
Log Mean (2)	8.35	8.26	8.29	8.19	8.27
Log Dev. (2)	0.122	0.139	0.102	0.114	0.119
p	0.135	0.467	0.581	0.804	–
q	0.865	0.533	0.419	0.196	–

TABLE VI Parameters for the bimodal lognormal model of the strength (MPa) of TITAO4 carbon fibre at different gauge lengths

Parameters	Gauge lengths (mm)				
	4.76	6.35	9.54	12.7	Average
Size	43	43	46	41	43
Log Mean (1)	7.90	7.76	7.82	8.98	7.86
Log Dev. (1)	0.124	0.098	0.185	0.139	0.137
Log Mean (2)	8.32	8.30	8.24	8.32	8.30
Log Dev. (2)	0.149	0.151	0.128	0.089	0.129
p	0.116	0.233	0.348	0.575	–
q	0.884	0.767	0.652	0.425	–

TABLE VII Gauge length dependence of the fibre strength parameters for the bimodal lognormal model

Strength parameters	F3UTUS	TDPO coated fibres
p	Independent of L, 0.48	$1 - aL^{-b}$
q	Independent of L, 0.52	aL^{-b}
Lognormal Mean, μ_i	$a_i - b_i$ [ln (L)]	Independent of L
Lognormal deviation, σ_i	Independent of L	Independent of L

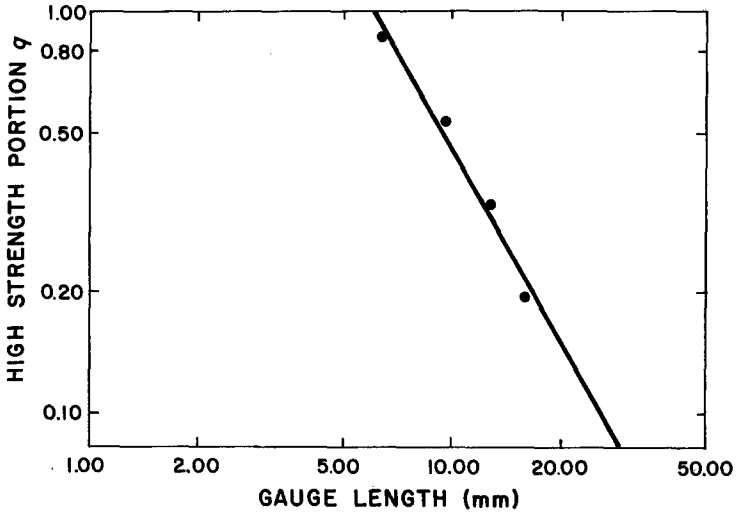

Figure 7 Weighting factors q for the high strength population as a function of gauge length in the bimodal lognormal model for the strength of TITAO2 carbon fibre.

Figure 8 Estimated distributions of fibre strength for F3UTUS (A) and electrocoated TITAO2 (B) carbon fibres.

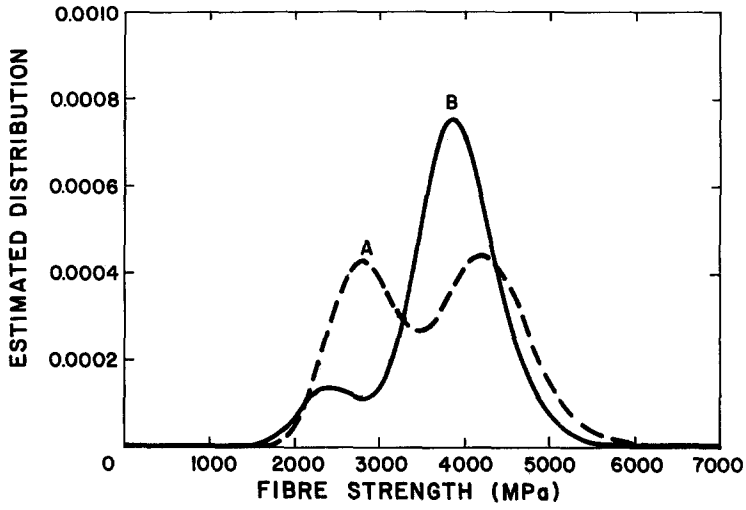

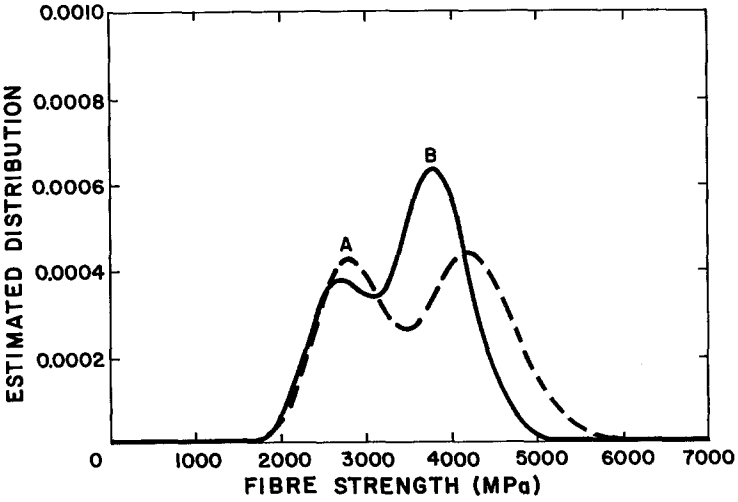

Figure 9 Estimated distributions of fibre strength for F3UTUS (A) and electrocoated TITAO3 (B) carbon fibres.

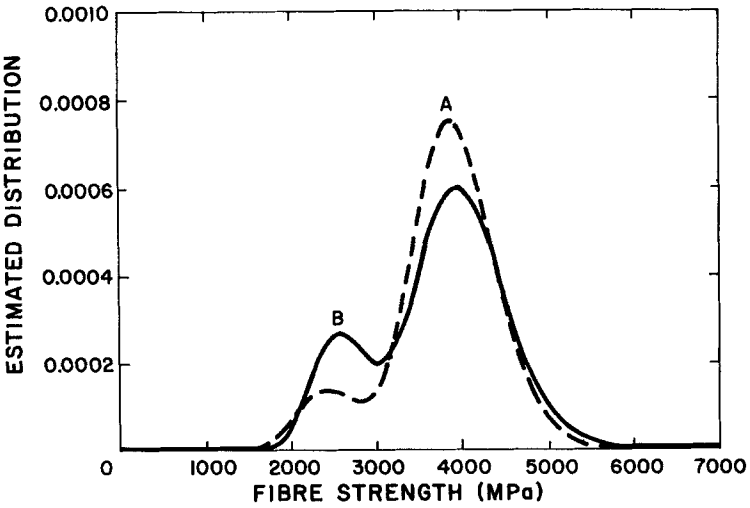

Figure 10 Estimated distributions of fibre strength for electrocoated TITAO2 (A) and TITAO4 (B) carbon fibres.

of the presence of both surface and internal flaws that cause failure. Since p is considerably reduced by surface coating, one can designate the type 1 flaws as the surface defects which are healed by the coating process. Also, writing the ratio

$$x = N_2G_2(l)/N_1G_1(l),$$

$$q = 1 - \frac{1}{1 + x}$$

and

$$\frac{dq}{dx} = \frac{1}{(1 + x)^2} > 0$$

i.e. q is a monotonically increasing function of x. Since q increases with gauge length after surface treatment (Fig. 6) the ratio x is also increased by the surface coating process. This increase can result from a decrease of the denominator of $N_1G_1(l)$ which can come about as follows: when the type 1 surface flaws are reduced by electrocoating, N_1 will be decreased; furthermore, the average interflaw spacing will be increased, and so $G_1(l)$ will also decrease.

That the effect of electrodeposition is not a mere sizing effect of the physical presence of coating is indicated by the observed changes in the values of p and q on washing off the electrodeposited coating. From Table IV, it is seen that p for TITAO2 at 6.35 mm gauge length is 0.135 whereas that for TITAO4, electrocoated under the same conditions but washed after the electrodeposition process is 0.233 at the same gauge length (Table VI). This increase in p, denoting an increase in the fraction of surface flaws, may be caused by removal of the protective layer of surface coating. However, the value of p for TITAO4 is still lower than that for untreated fibre, which is 0.48 (Table VII). It is possible that the electrodeposition process is also accompanied by electrochemical oxidation of the anodic carbon fibres, with etching away or blunting of surface flaws or defects.

Furthermore, it can be seen from the higher value of p for TITAO3 (Table V) compared to TITAO4 that the electrochemical oxidation, at much higher current and voltage conditions adopted for this set, can cause more and/or more severe flaws on the fibre surface. Variations in fibre–matrix adhesion for these fibres, discussed in another paper [8], also indicate the occurrence of electrochemical oxidation as a side reaction.

The trends in gauge length sensitivity for the coated fibres supports the above reasoning. From Equation 1, and using the appropriate values of a and b, one can estimate the length at which the high strength population fraction q reaches one. Thus, for TITAO2, TITAO4 and TITAO3, q is 1 at 6.04, 4.23 and 3.11 mm respectively, supporting the inference that in coated unwashed fibres, surface flaws are rendered ineffective at larger gauge lengths than in coated, washed fibres (TITAO4 and TITAO3). The formation of new flaws by electrochemical oxidation at more drastic conditions is also consistent with the above trend.

It was noted earlier (Tables IV to VII) that in contrast to the dependence of the respective weighting factors p and q for the low and high strength populations, the lognormal means μ_1 and μ_2 for the two modes were essentially unchanged with gauge length. The constancy of μ_1 and μ_2 over the tested gauge length region is an indication that the severities of the flaws for the two populations are unaffected by sampling (gauge length) or end effects, because each mode is truly independent in the range of tested gauge lengths. While this seems to be true for the electrocoated fibres (TITAO2, TITAO3, and TITAO4), indications are otherwise for the untreated fibre (F3UTUS, Fig. 5). Here, the slight increase in lognormal mean for both modes even at the lower gauge lengths suggests that the flaws may vary in type and severity within each mode. Thus, in spite of the better fit of the bimodal lognormal model to the strength data, it is quite likely that a multimodal failure model would be more accurate for the untreated fibre.

TABLE VIII Parameters of the bimodal lognormal model of fibre strengths

Parameters	F3UTUS	TITAO2	TITAO3	TITAO4
Log Mean (1)	7.96	7.82	7.92	7.86
Log Dev. (1)	0.156	0.161	0.158	0.137
Log Mean (2)	8.36	8.27	8.26	8.30
Log Dev. (2)	0.117	0.119	0.103	0.129
Exp (Log Mean 1)	2860	2480	2760	2610
Exp (Log Mean 2)	4280	3910	3850	4010

The lognormal parameters are summarized in Table VIII. The values were calculated from data at the lowest tested gauge lengths, 4.76 mm for TITAO3 and TITAO4, and 6.35 mm for TITAO2. For F3UTUS the average of values for 4.76 to 12.7 mm was used. An interesting feature emerges on comparing the exponentials of the lognormal means in the last two rows. It can be seen that the mean values for each mode are reduced slightly for the electrocoated fibres. This would indicate that the upper portion of the lower strength population in the untreated fibre is shifted, after electrocoating, to the lower portion of the higher strength population. The type of flaws characterizing p and q fractions in the treated fibre may not, therefore, be the same as in the untreated fibre.

5. Conclusions

A bimodal lognormal model fits the tensile strength distribution of PAN-based Fortafil 3 fibres. The model is consistent with the presence of flaws of two types, surface flaws and internal defects, in the untreated fibre. Both have the same structural origin which may be associated with misoriented crystallites. The surface flaws constituting the weaker population are reduced by electrodeposition of TDPO under mild conditions which thus increases the proportion of high strength population. The conditions of electrodeposition need to be controlled carefully to avoid the formation of new or severe surface flaws by concurrent electrochemical processes.

Acknowledgements

Support of this research through grants from the Boeing Company and the WSU Grant-in-aid Program is gratefully acknowledged.

References

1. D. A. SCOLA, in "Interfaces in Polymer Matrix Composites", edited by E. P. Plueddemann (Academic Press, New York, 1974) Ch. 7.
2. P. EHRBURGER and J. B. DONNET, *Phil. Trans. R. Soc. London* **A294** (1980) 495.
3. R. V. SUBRAMANIAN, *Pure Appl. Chem.* **52** (1980) 1929.
4. R. V. SUBRAMANIAN and J. J. JAKUBOWSKI, *Polym. Eng. Sci.* **18** (1978) 590.
5. *Idem., Composites* **11** (1980) 161.
6. J. J. JAKUBOWSKI and R. V. SUBRAMANIAN, US Pat. 4272346 (1981).
7. SHI-HAU OWN, PhD thesis, Washington State University (1984).
8. SHI-HAU OWN, R. V. SUBRAMANIAN and S. C. SAUNDERS, in preparation.
9. R. D. SCHILE and G. A. RASICA, *Rev. Sci. Instrum.* **38** (1967) 1103.
10. M. H. DEGROOT, "Probability and Statistics" (Addison-Wesley, Menlo Park, California, 1975).
11. W. W. HINES and D. C. MONTGOMERY, "Probability and Statistics in Engineering and Management Science" (John Wiley, New York, N.Y., 1980).
12. W. WEIBULL, *J. Appl. Mech.* **18** (1951) 293.
13. S. CHWASTIAK, J. B. BARR and R. DIDCHENKO, *Carbon* **17** (1979) 49.
14. J. W. HITCHON and D. C. PHILLIPS, *Fibre Sci. Technol.* **12** (1979) 217.
15. C. P. BEETZ Jr, *ibid.* **16** (1982) 45.
16. E. G. KENDALL, in "Metallic Matrix Composites", edited by K. G. Kreider (Academic Press, New York, 1974) p. 333.
17. S. C. BENNETT, D. J. JOHNSON and W. JOHNSON, *J. Mater. Sci.* **18** (1983) 3337.

Received 10 July 1985
and accepted 21 January 1986